Microchemical Journal 190 (2023) 108738

Contents lists available at ScienceDirect

Microchemical Journal

journal homepage: www.elsevier.com/locate/microc

Wine age prediction using digital images and multivariate calibration

Olga Vyviurska [a], Liudmyla Khvalbota [a], Nemanja Koljančić [a], Ivan Špánik [a,*], Adriano A. Gomes [a,b,*]

[a] Institute of Analytical Chemistry, Faculty of Chemical and Food Technology, Slovak University of Technology in Bratislava, Radlinského 9, 812 37 Bratislava, Slovakia
[b] Instituto de Química, Universidade Federal do Rio Grande do Sul, Avenida Bento Gonçalves, 9500, 91501-970 Porto Alegre, RS, Brazil

ARTICLE INFO

Keywords:
Botrytized wine
Age prediction
Colour histogram
Partial least square regression
Wine quality control

ABSTRACT

The prediction or confirmation of age is an important field in evaluation of wine's value. Such type of studies commonly requires a number of data sets describing changes in chemical composition and/or related physical properties. Digital images of wines captured by a webcam represent an easy and low-cost approach to prevent frauds connected to the age of wines. In this work, a combination of frequency histograms including grey scale, red-green-blue (RGB) and hue-saturation-value (HSV) colour models extracted from digital images were used to evaluate the age of botrytized and related varietal wines produced during a 1989–2019 period at different countries. The main findings showed that digital images carry the appropriate chemical information for the age assignment and PLS-type models were able to estimate wine age only one latent variable. Grey levels enabled to find figure of merit values similar to the PLS model based on full histogram. An additional interval selection of the histograms with interval PLS allows improving accuracy of variable assessment and achieving lower error at a cross-validation step, RMSECV decreases from 3.6 years to 3.1 years. When models were employed to predict an external set of samples similar results were found, RMSEP equal to 2.8 years and 2.9 years for PLS and *i*PLS, respectively. However, a slight deterioration of the results was observed for the PLS model based on full grey levels (RMSEP 3.2). In general, these non-destructive measurements do not generate residuals and can be performed without sophisticated equipment with a reasonably accurate response.

1. Introduction

Wine vintage and aging period belong to crucial factors influencing prices of high-quality wine [1]. This is consistent with higher costs of longer wine maturation especially in the wood barrels [2,3]. Furthermore, an increase in wine prices is typically observed for bad vintages with lower distribution of the wine on the market [4]. During oxidative aging in barrels, some biochemical processes occur like anthocyanin and tannin polymerization, as well as phenolic compounds exchange between wood and wine [5–7]. Considering a large number of fraudulent acts in the areas of food and beverage industry, composition data are especially useful in identifying frauds and adulterations [8,9]. A few studies have been published on prediction of the age of wines, based on chemical composition of wine (e.g. organic acid content, furanoids, phenolic and volatile compounds) [10–13], or spectroscopic analysis including UV–Vis and infrared spectrometry, especially in the near-IR range [14–16], and a voltammetric electronic tongue [17].

In the context of food analysis, digital images have been reported in the literature for different purposes [18]. As to wine analysis, digital image data were used to establish geographic origin, winemaker, and grape type [19], to detect adulterations in aged wine [20]. A colorimetric sensor array was also tested for classification of rice wine according to different marked ages [21]. However, this study was mainly focused on screening analysis, rather than on the sample age prediction. Overall colour information extracted from a digital image can be expressed through an average value or described with univariate models based on the calibration line [22]. Use of full histograms is more frequent [18], and it provides multivariate data suitable for processing with several chemometric tools. Besides wine analysis, a combination of chemometric tools and digital imaging was exploited for food samples and other types of samples. The selected chemometric approaches could include more traditional tools, like component analysis (PCA), linear discriminant analysis (LDA), partial least squares - discriminant analysis (PLS-DA), partial least squares (PLS), as well as more complex methods

* Corresponding authors at: Institute of Analytical Chemistry, Faculty of Chemical and Food Technology, Slovak University of Technology in Bratislava, Radlinského 9, 812 37 Bratislava, Slovakia (Adriano A. Gomes).
E-mail addresses: ivan.spanik@stuba.sk (I. Špánik), araujo.gomes@ufrgs.br (A.A. Gomes).

https://doi.org/10.1016/j.microc.2023.108738
Received 12 December 2022; Received in revised form 3 April 2023; Accepted 5 April 2023
Available online 10 April 2023

such as back-error propagation-artificial neural network (BP–ANN), support vector machines (SVM), random forest, among others [18–21].

In this study, a combination of frequency histograms including grey scale, red-green-blue (RGB) and hue-saturation-value (HSV) colour models extracted from digital images were used to evaluate the age of botrytized and related varietal wines produced during a 1989–2019 period at different countries. This study presents a quick, cheap and highly accurate approach based on frequency histograms extracted from digital images for age prediction of different types of white wines.

2. Materials and methods

2.1. Samples

Forty-seven wine samples produced from 1989 to 2019 in Slovakia (28), Hungary (4), Ukraine (2), France (5) and Austria (8) were selected for evaluation. A list of all the studied samples with labelling, classification and vintage year is shown in Table 1S. The samples included botrytized wines and related varietal wines (Furmint, Lipovina, Muscat grape varieties, Sauvignon Blanc and Semillon, Chardonnay, Weissburgunder, Welschriesling), which were authentic and obtained directly from the producers. The wines were stored in glass bottles at 4 °C. After opening a 20 mL wine aliquot was transferred into a vial and equilibrated at 20 °C before image acquisition.

2.2. Instrumentation

A white cardboard box equipped with a webcam (see Fig. 1S the schematic diagram of the homemade system) was designed to acquire digital images under the controlled conditions. The WC040 MULTILASER webcam with glass lenses and a USB connector were fixedly positioned at a distance of 15 cm from the sample at 180°angle with respect the samples. The equipment was operated under the following conditions: Frame rate: 28 FPS; Picture mode: RGB; MegaPixels Webcam: 0.31 MP; Webcam Resolution: 640 × 480; Screen Aspect Ratio: 1.33; JPEG file size: 268.03 kB; Bitrate: 7.3 MB/s; Number of colours: 55071; Lightness: 57.84%; Brightness: 59.10%; Brightness: 57.65%; Hue: 143 and Saturation: 6.05%. This image acquisition system was previously used in [23]. The acquired images were saved in a laptop computer as a JPEG file format and processed in a MatLab 2019b environment. The grayscale, red-green-blue (RGB) and Hue-Saturation-Value (HSV) features were extracted by ImageGUI interface [24]. A set of data arranged in a 47 × 1792 array that was subsequently submitted to chemometric treatments. A row of the array corresponds to the sample and the column to a colour level intensity.

2.3. Data analysis

An elliptical central area corresponding to a region of interest (ROI) was selected automatically and used for extraction of the histogram. Various colour models and parameters can be exploited to process digital images for development of analytical methods [18]. In order to avoid excessively redundant information and/or to generate a too large data matrix, in this case, red-green-blue (RGB) and Hue-Saturation-Value (HSV) colour models were considered as efficient colour descriptors of the samples. Once that picture was stored in 24 bits format, 256 colour levels is possible in a range of from 0 to 255 in each colour channel. Thus, each sample was represented by a 1 × 1792 row vector. At the preliminary evaluation step, PCA was performed on the set of 47 mean centred histograms and this pre-processing strategy was used for all cases at the later modelling steps in the calibration phase. To build multivariate models for prediction of wine age, the initial data set was partitioned into a calibration set ($\mathbf{X_{cal}}$ sized 30 × 1792) and an external prediction set ($\mathbf{X_{pred}}$ sized 17 × 1792) by means of a *SPXY* algorithm (Sample set Partitioning based on joint **x**–*y* distances) [25]. Model dimensionality was optimised based on the calibration set by leave one out cross validation (LOOCV) and Monte Carlo (MC) approach [26], which used ten cycles with 70% of the samples retained for calibration. Estimation of a suitable number of latent variables was carried out by means of Haaland and Thomas criterion [27]. Errors in LOOCV are subjected to a Fisher *F*-test in order to check the presence of outliers. The PLS model was improved by a variable selection using two different strategies, such as intervals-PLS (*i*PLS) algorithm [28] and intervals Successive Projection Algorithm coupled to PLS model (*i*SPA-PLS) [28–29]. Intervals with different widths (from 5 to 75) were compared with each other and the full PLS model (indicated as a zero interval). The models were assessed with square errors of calibration (RMSEC), validation (RMSECV) and prediction (RMSEP). Relative prediction error (REP), determination coefficient (R^2) and presence of systematic error (bias) were also considered.

All calculations were performed in a MatLab 2019b environment. Histograms extracted from DI and the sample set partition by SPXY algorithm were processed according to homemade routines (available at http://www.ccen.ufpb.br/laqa/index.php/downloads) [24]. PCA calculation was performed using PCA Toolbox 1.5 available at https://michem.unimib.it/ [30]. PLS and *i*PLS models including validation by LOOCV and MC were evaluated using MVC1 [26] (available at https://www.iquir-conicet.gov.ar/eng/div5.php?area=12) graphical interfaces. *i*SPA-PLS was calculed using the VSTOOLBOX GUI.

3. Results

3.1. Data set and general comments

Fig. 1a presents a typical digital image of wine (DI) included in this study. An elliptical central area corresponds to a region of interest (ROI) was used for extraction of a histogram (Fig. 1b). Red-green-blue (RGB) and Hue-Saturation-Value (HSV) colour models were considered for processing of data. As can be seen at Fig. 1b, a colour histogram shows too narrow peaks at the grey scales, all channels of the RGB model and Value (V) range. On the other hand, hue and saturation channels show a wide dispersion with non-null values for most colour levels.

Spectrophotometric evaluation of wine aging is commonly based on measurement of absorbance at 420 nm and 520 nm. A decrease in absorbance at 520 nm and an increase of absorbance at 420 nm are related to transformation of monomeric anthocyanins into polymeric forms during aging process [31]. In our case, it could be also responsible for a bimodal character of the histograms (Fig. 1b). In order to predict wine vintage, the average colour value of each channel was plotted against wine age (Fig. 2). A change of wine colour is clearly observed over a 20-year period (the bottom right corner of Fig. 2), which supports digital image evaluation in the study.

Generally, not all average colour channels showed a correlation between the average values and age of the wines. The distribution pattern of the parameters was more prominently observed only for Grey scale and Green. In addition, the samples used in the study show colours that are described like red-orange tones, which are complementary to shades of green. Therefore, it is reasonable that these colour models could closely match wine colour variations with age. Grey scale represents a range of monochromatic shades from black to white that is computed of the RGB model, so the information observed in the green levels is also present in the grey scale. Furthermore, in the HSV colour model the most promising correlation was observed between Value (V) and wine age was observed. According to hue-oriented colour space of the HSV model, it is related to brightness or intensity of light present in the colour. HSV can be easily obtained from the RGB colour space using equations described in [32], where it is possible to see that a relationship between the Value of the HSV model and the RGB is more direct compared to the H and S channels. At this point, all three colour models (Grey scale, RGB and HSV) show useful information for age prediction of wine samples.

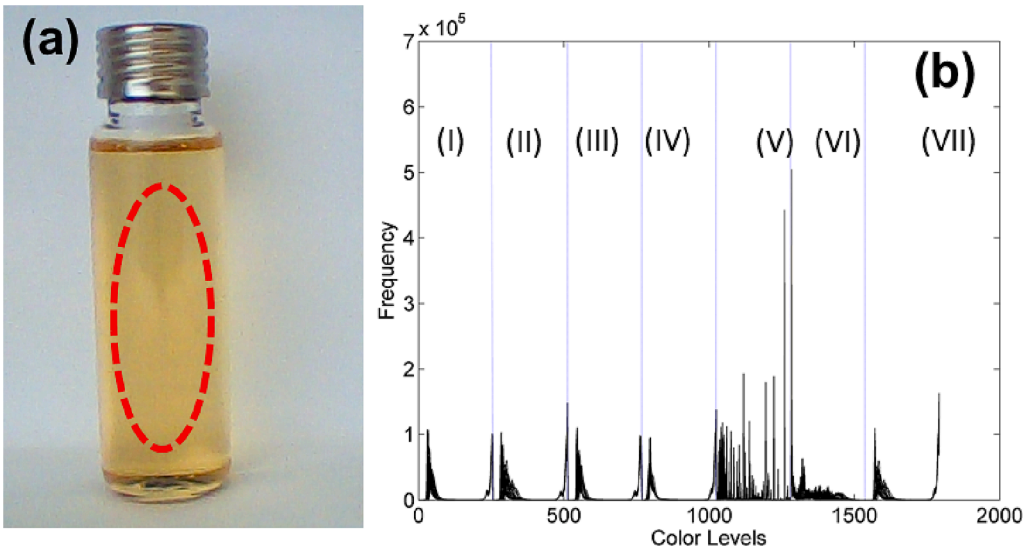

Fig. 1. Wine data: (a) typical DI and ROI, (b) histograms for all the samples. Where the regions identified from I to VII correspond to Grey scale, Red, Green, Blue, hue, Saturation and Value respectively. (For interpretation of the references to colour in this figure legend, the reader is referred to the web version of this article.)

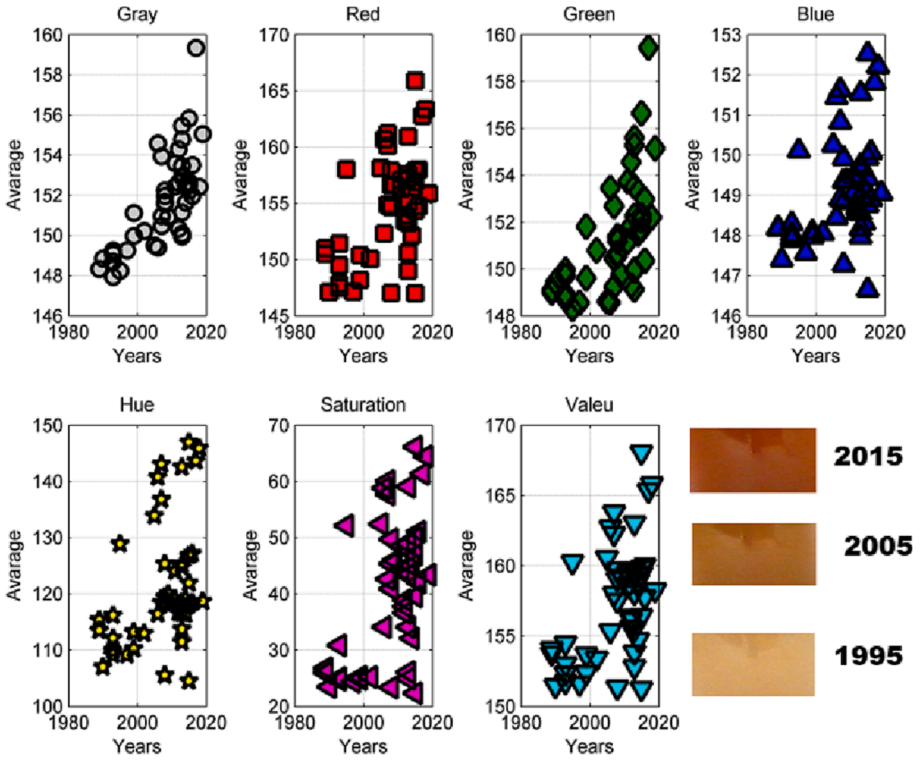

Fig. 2. A correlation plot between the average colour value against wine samples age.

3.2. Exploratory analysis by PCA

In order to perform a preliminary exploratory analysis, PCA was carried out for all the samples to find any pattern linked to wine age. The results can be visualized on a two dimensional (PC1 × PC2) score plot (see Fig. 2S). The first two principal components exhibit a cumulative variance of approximately 60% of all sources of variance in the dataset. Information related to the age of the wine plays an important source of variability in digital images associated with PC1. Note that the youngest samples are primarily located in the region of negative PC1 scores, whereas the samples of intermediate age could be found near zero values of PC1 and the oldest samples exhibit positive PC1 scores. These results suggest that digital images represent chemical information associated with wine age and could be exploited for that predictive purpose. In addition, no sample was characterised with anomalous behaviour, suggesting the absence of an outlier in the dataset.

3.3. Calibration, interval selection and prediction

Afterwards the PLS model was fitted on calibration data set using one LV. A single LV corresponds to the minimum on the curve of RMSECV *vs.* the number of latent variables included in the PLS model estimated by both LOOCV and MC strategies, indicating a convergence between both approaches (see Fig. 3S). As can be seen in Fig. 3a, no outlier was

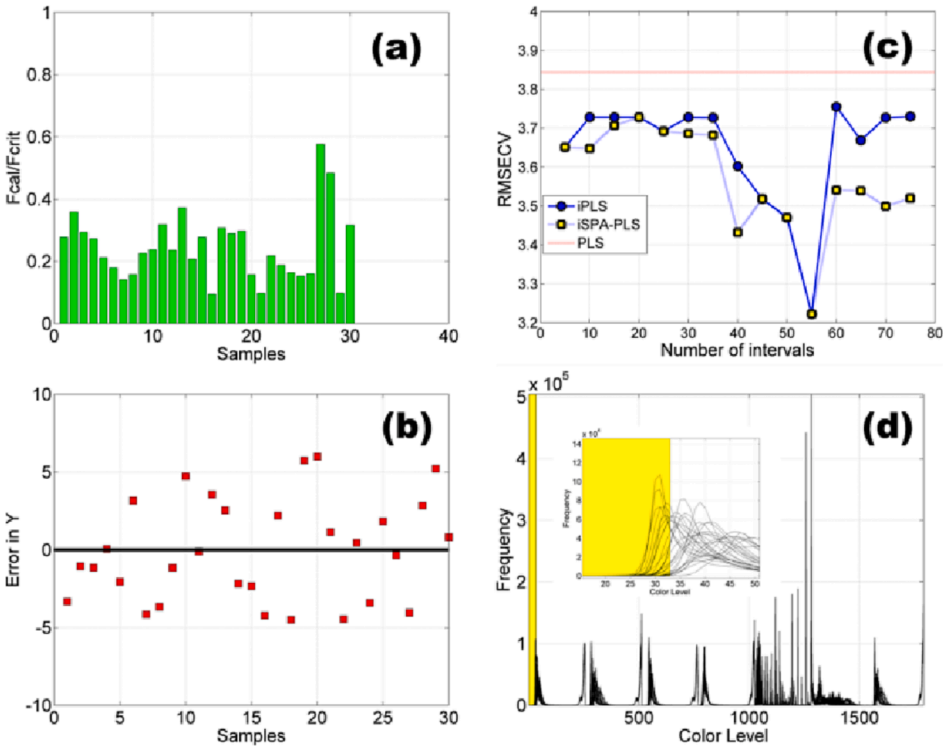

Fig. 3. Optimization of PLS multivariate models: (a) outlier detection computed by CV, (b) residuals in y calculated by CV, (c) interval width *vs.* MSECV and (d) the selected interval by both *i*SPA-PLS and *i*PLS.

detected in calibration set according to *F* test with 95% of statistic confidence. The visual inspection of **y** residuals estimated by LOOCV (see Fig. 3b) showed absence of a nonlinearity between histograms and wine age. In addition it was also confirmed by Durbin-Watson Test.

In order to improve the PLS model, a variable selection of DI histogram intervals was performed with two different approaches, such as intervals-PLS (*i*PLS) Algorithm and intervals Successive Projection Algorithm coupled to PLS model (*i*SPA-PLS). Histograms were divided into different numbers of intervals (Fig. 3c), and were compared with each other and also to the full PLS model (indicated by a horizontal red line). As a result, some interesting findings could be highlighted in this case. All interval selection based models shows better accuracy in comparison to the PLS model. In general, the better results were obtained with *i*SPLA-PLS models, however the optimum number of intervals (55) was obtained by both variable selection strategies. The selected region was a narrow interval containing only the first 33 Gy scale values which is highlighted in yellow in Fig. 3d. Considering that only one interval in the greyscale zone was selected, the PLS model for the entire region with 256 colours levels was calculated and the results compared to the other PLS models. Since the *i*PLS and *i*SPA-PLS models provided the same result, only the results for the *i*PLS will be displayed. The observed convergence is related to particular implementation of these methods. In the case of the *i*PLS calculations, the number of intervals *w* is defined by the user and only one interval among the *w* is selected. The number of intervals *w* is also set up at the first stage for the *i*SPA-PLS model, however an interval range from 1 to *w*-1 is available for further data processing. It is defined by the projection criteria of vectors (more details can be found in [29]) and such selection of the subset of intervals allows to minimize the CV error. In specific cases, where the best subset of intervals corresponds to one interval, *i*PLS and *i*SPA-PLS should show the same result.

As can be seen from Table 1, small prediction errors were found in both steps (calibration and cross validation), indicating a good fitness between themselves. These results confirm a proper selection of one LV with the LOOCV and MC procedures. Comparing the PLS and *i*PLS models based on the range selection, we could observe an improvement in accuracy with a variable selection approach. However, the PLS model based on the use of the entire range of grey scale colour levels did not show significant improvements compared to the PLS model based on full histogram. The most efficient models for predicting the age of wine samples were obtained from grey, green and value scale and based on average calculations (see Fig. 2). The interval selections performed by two different approaches showed a convergence to a same narrow region belong to grey scale zone. Inspection of the Pearson correlation coefficient (*r*) between each ash level and the age of the wines (Fig. 4S) reveals that both interval selection methods highlighted the range with the highest *r* values. The plots of the values predicted in cross-validation and for the test set *vs.* actual wine age are shown in Fig. 4 for both PLS and *i*PLS models.

Table 1
Statistical summary of calibration and cross-validation.

Models	LV	RMSEC (years)	REP (%)	R^2_{cal}	RMSECV (years)	REP_{CV}(%)	R^2_{cv}
PLS	1	3.6	0.18	92.18	3.8	0.19	90.22
Grey-PLS	1	3.5	0.18	92.31	3.7	0.19	90.71
***i*PLS**	1	3.1	0.16	94.10	3.2	0.16	93.21

The predicted values are distributed along the bisector of the predicted *vs.* actual plot without positive or negative trends, that are in agreement with the values of figures of merit shown in Table 1. All models were applied in the prediction of the independent set of samples and the results are summarized in Table 2.

An *F*-test showed no outlier in prediction set (Figs. 5S, 6S and 7S). The good agreement between predicted and actual values can be seen also in both Table 2 and Fig. 4. Overall, *i*PLS showed improvements for calibration and cross-validation in comparison to the full model PLS.

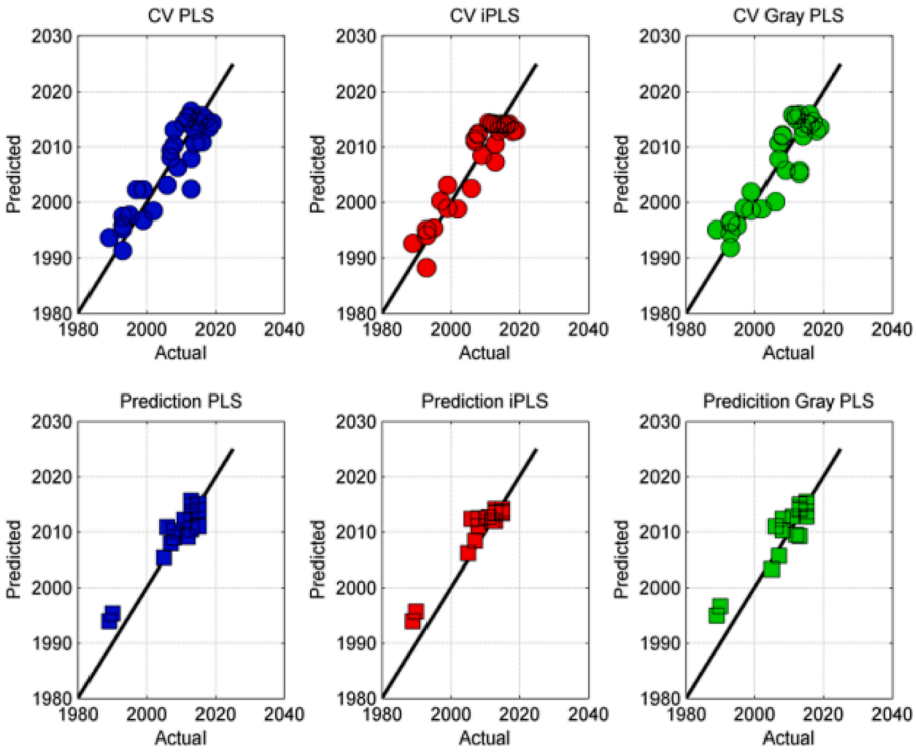

Fig. 4. Actual versus estimated wine age for all model in both cross validation and prediction step.

Table 2
Statistical summary of prediction. Bias test *t*-test at 95% Statistical confidence t_{crit} 1.7459.

Models	**PLS**		**iPLS**		**Gray-PLS**	
RMSEP	2.80		2.90		3.20	
REP	0.14		0.14		0.16	
R^2	95.61		93.36		96.61	
bias	absent (tcal = 1.1676)		absent (tcal = 1.5439)		absent (tcal = 1.5439)	
Acutual	**Predicted**	**SD**	**Predicted**	**SD**	**Predicted**	**SD**
2015	2011	0.4	2014	0.8	2013	0.6
2008	2009	0.3	2013	0.7	2012	0.6
1990	1995	0.9	1996	1.0	1997	0.9
2013	2016	0.8	2014	0.8	2015	0.8
1989	1994	1.0	1994	1.1	1995	0.9
2012	2009	0.3	2012	0.7	2010	0.4
2015	2015	0.7	2014	0.8	2015	0.8
2011	2012	0.5	2013	0.7	2013	0.6
2015	2015	0.7	2014	0.8	2016	0.8
2013	2014	0.6	2013	0.8	2014	0.8
2013	2015	0.7	2014	0.8	2014	0.7
2008	2010	0.4	2011	0.7	2010	0.5
2015	2014	0.6	2013	0.8	2014	0.7
2005	2005	0.3	2006	0.6	2003	0.5
2006	2011	0.4	2012	0.7	2011	0.5
2013	2011	0.4	2012	0.7	2009	0.4
2007	2008	0.2	2008	0.6	2006	0.4

4. Conclusion

Visual inspection of the plots reporting the correlations of the age of the wines with the average colour values in each channel (grey scale, G in RGB and Value in HSV) showed encouraging preliminary results. The obtained digital images were modelled by PLS as well as PLS coupled with the interval selection. The last strategy shows improvement with respect to the full model at the calibration and cross-validation stages. However, in the case of the production of an independent set of samples, similar results were achieved for all cases. Although the sample set included different types of producers and technological production processes and also from different countries, age information could be modelled and predicted by PLS. This proposed approach appears as an alternative and useful tool for an analysis and screening of this important parameter of the wine market. It requires only a homemade system of a cardboard box with a white background and controlled lighting combined with a webcam. It is noteworthy that every procedure, in addition to being low cost, does not generate waste, complying with the sustainability guidelines of green chemistry. Last but not least, the combined simplicity of PLS and digital images opens up a series of possibilities for determining the age of wines through on-site analysis, since the proposed method can be adapted to the use of mobile devices such as smart phones.

CRediT authorship contribution statement

Olga Vyviurska: Methodology, Writing – original draft, Writing – review & editing. **Liudmyla Khvalbota:** Investigation, Methodology, Writing – original draft. **Nemanja Koljančić:** Methodology, Writing – original draft, Writing – review & editing. **Ivan Špánik:** Conceptualization, Writing – original draft, Writing – review & editing, Funding acquisition, Supervision, Project administration. **Adriano A. Gomes:** Methodology, Writing – original draft, Writing – review & editing.

Declaration of Competing Interest

The authors declare that they have no known competing financial interests or personal relationships that could have appeared to influence the work reported in this paper.

Data availability

The authors do not have permission to share data.

Acknowledgement

This project has received funding from Slovak Research and Development Agency under Contract No. APVV-21-0211 and the European Unioń s Horizon 2020 research and innovation programme under the Marie Skłodowska-Curie grant agreement No 945478. Dr. Gomes A. A. is thankful to CNPq for you fellowship (313381/2021-6) and Universal grants (438734/2018-1). Liudmyla Khvalbota and Nemanja Koljančić would like to thank for financial contribution from the STU Grant scheme for Support of Young Researchers (OPTAL and KOMBI) and STU Grant scheme for Support of Excellent Creative Teams of Young Researchers (SOLUTION).

Appendix A. Supplementary data

Supplementary data to this article can be found online at https://doi.org/10.1016/j.microc.2023.108738.

References

[1] S. Du, Y. Chen, J. Peng, T. Nie, Incorporating risk fairness concerns into wine futures under quality uncertainty, Omega 113 (2022), 102717, https://doi.org/10.1016/j.omega.2022.102717.
[2] A.M. Angulo, J.M. Gil, A. Gracia, M. Sánchez, Hedonic prices for Spanish red quality wine, Br. Food J. 120 (2000) 481–493, https://doi.org/10.1108/00070700010336445.
[3] J.L. Breeden, How sample bias affects the assessment of wine investment returns, JWE 17 (2022) 127–140, https://doi.org/10.1017/jwe.2022.20.
[4] M. Sánchez, J.M. Gil, Consumer preferences for wine attributes in different retail stores: a conjoint approach, Int. J. Wine Mark. 10 (1998) 25–38, https://doi.org/10.1108/eb008675.
[5] M. Carpena, A.G. Pereira, M.A. Prieto, J. Simal-Gandara, Wine aging technology: fundamental role of wood barrels, Foods 9 (2020) 1160, https://doi.org/10.3390/foods9091160.
[6] D. Hernanz, V. Gallo, Á.F. Recamales, A.J. Meléndez-Martínez, M.L. González-Miret, F.J. Heredia, Effect of storage on the phenolic content, volatile composition and colour of white wines from the varieties Zalema and Colombard, Food Chem. 113 (2009) 530–537, https://doi.org/10.1016/j.foodchem.2008.07.096.
[7] C. Ubeda, Á. Peña-Neira, M. Gil i Cortiella, Combined effects of the vessel type and bottle closure during Chilean Sauvignon Blanc wine storage over its volatile profile, Int. Food Res. J. 156 (2022), 111178, https://doi.org/10.1016/j.foodres.2022.111178.
[8] H. Yu, B. Ying, T. Sun, X. Niu, X. Pan, Vintage year determination of bottled Chinese rice wine by VIS-NIR spectroscopy, J. Food Sci. 72 (2007) E125–E159, https://doi.org/10.1111/j.1750-3841.2007.00308.x.
[9] L. Holmberg, Wine fraud, Int. J. Wine Res. 2 (2010) 105–113, https://doi.org/10.2147/IJWR.S14102.
[10] D.A. Guillén, M. Palma, R. Natera, R. Romero, C.G. Barroso, Determination of the age of sherry wines by regression techniques using routine parameters and phenolic and volatile compounds, J. Agric. Food Chem. 53 (2005) 2412–2417, https://doi.org/10.1021/jf048522b.
[11] I. Dos Santos, G. Bosman, J.L. Aleixandre-Tudo, W. du Toit, Direct quantification of red wine phenolics using fluorescence spectroscopy with chemometrics, Talanta 236 (2022), 122857, https://doi.org/10.1016/j.talanta.2021.122857.
[12] X. Chen, Z. Wang, Y. Li, Q. Liu, C. Yuan, Survey of the phenolic content and antioxidant properties of wines from five regions of China according to variety and vintage, LWT 169 (2022), 114004, https://doi.org/10.1016/j.lwt.2022.114004.
[13] Z. Wang, L. Zhang, Y. Li, Q. Liu, C. Yuan, Non-acylated and acylated anthocynins in red wines of different ages: Color contribution and evaluation, J. Food Compost. Anal. 115 (2023), 104951, https://doi.org/10.1016/j.jfca.2022.104951.
[14] R. Rendall, A.C. Pereira, M.S. Reis, Advanced predictive methods for wine age prediction: Part I-A comparison study of single-block regression approaches based on variable selection, penalized regression, latent variables and tree-based ensemble methods, Talanta 171 (2017) 341–350, https://doi.org/10.1016/j.talanta.2016.10.062.
[15] M.P. Campos, R. Sousa, A.C. Pereira, M.S. Reis, Advanced predictive methods for wine age prediction: Part II–A comparison study of multiblock regression approaches, Talanta 171 (2017) 132–142, https://doi.org/10.1016/j.talanta.2017.04.064.
[16] M. Basalekou, C. Pappas, Y. Kotseridis, P.A. Tarantilis, E. Kontaxakis, S. Kallithraka, Red wine age estimation by the alteration of its color parameters: Fourier transform infrared spectroscopy as a tool to monitor wine maturation time, J. Anal. Methods Chem. 2017 (2017) 1–9.
[17] Z. Wei, J. Wang, L. Ye, Classification and prediction of rice wines with different marked ages by using a voltammetric electronic tongue, Biosens. Bioelectron. 26 (2011) 4767–4773, https://doi.org/10.1016/j.bios.2011.05.046.
[18] P.H.G.D. Diniz, Chemometrics-assisted color histogram-based analytical systems, J. Chemom. 34 (2020) e3242, https://doi.org/10.1002/cem.3242.
[19] C.M. Lima, D.D.S. Fernandes, G.E. Pereira, A.A. Gomes, M.C.U. Araújo, P.H.G. D. Diniz, Digital image-based tracing of geographic origin, winemaker, and grape type for red wine authentication, Food Chem. 312 (2020), 126060, https://doi.org/10.1016/j.foodchem.2019.126060.
[20] C. Herrero-Latorre, J. Barciela-García, S. García-Martín, R.M. Peña-Crecente, Detection and quantification of adulterations in aged wine using RGB digital images combined with multivariate chemometric techniques, Food Chem.: X 3 (2019), 100046, https://doi.org/10.1016/j.fochx.2019.100046.
[21] Q. Ouyang, J. Zhao, Q. Chen, H. Lin, Classification of rice wine according to different marked ages using a novel artificial olfactory technique based on colorimetric sensor array, Food Chem. 138 (2013) 1320–1324, https://doi.org/10.1016/j.foodchem.2012.11.124.
[22] J. H. Santos Neto, I. S.A. Porto, M. P. Schneider, A. M.P. dos Santos, A. A. Gomes, S. L.C. Ferreira. Speciation analysis based on digital image colorimetry: Iron (II/III) in white wine. Talanta 194 (2019) 86-89. https://doi.org/10.1016/j.talanta.2018.09.102.
[23] A. Araújo, W. Marinho, A. de Araújo Gomes, A fast and inexpensive chemometric-assisted method to identify adulteration in acai (Euterpe oleracea) using digital images, Food Anal. Methods 11 (7) (2018) 1920–1926, https://doi.org/10.1007/s12161-017-1127-4.
[24] D. Douglas de Sousa Fernandes, V.E. Almeida, L. Pinto, G. Véras, R.K. Harrop Galvão, A.A. Gomes, M.C. Ugulino Araújo, The successive projections algorithm for interval selection in partial least squares discriminant analysis, Anal. Methods 8 (41) (2016) 7522–7530, https://doi.org/10.1039/C6AY01840H.
[25] R.K.H. Galvão, M.C.U. Araujo, G.E. José, M.J.C. Pontes, E.C. Silva, T.C.B. Saldanha, A method for calibration and validation subset partitioning, Talanta 67 (2005) 736–740, https://doi.org/10.1016/j.talanta.2005.03.025.
[26] F.A. Chiappini, H.C. Goicoechea, A.C. Olivieri, MVC1_GUI: A MATLAB graphical user interface for first-order multivariate calibration. An upgrade including artificial neural networks modelling, Chemom. Intell. Lab. Syst. 206 (2020) 104162, https://doi.org/10.1016/j.chemolab.2020.104162.
[27] R.K.H. Galvão, M.C.U. Araújo, W.D. Fragoso, E.C. Silva, G.E. José, S.F.C. Soares, H. M. Paiva, A variable elimination method to improve the parsimony of MLR models using the successive projections algorithm, Chemom. Int. Lab. Systm. 92 (2008) 83–91, https://doi.org/10.1016/j.chemolab.2007.12.004.
[28] L. Norgaard, A. Saudland, J. Wagner, J. P. Nielsen, L. Munck, and S. B. Engelsen. Interval partial least-squares regression (iPLS): A comparative chemometric study with an example from near-infrared spectroscopy. Appl. Spectrosc. (2000) 54(3), 413-419 https://opg.optica.org/as/abstract.cfm?URI=as-54-3-413.
[29] A.A. Gomes, R.K.H. Galvão, M.C.U. Araújo, G. Véras, E.C. Silva, The successive projections algorithm for interval selection in PLS, Microchem. J. 110 (2013) 202–208, https://doi.org/10.1016/j.microc.2013.03.015.
[30] D. Ballabio, V. Consonni, Classification tools in chemistry. Part 1: linear models. PLS-DA, Anal. Methods 5 (16) (2013) 3790–3798, https://doi.org/10.1039/C3AY40582F.
[31] F.F. Heredia, M. Guzman-Chozas, The color of wine. A historical perspective. I Spectral evaluation, J Food Qual. 16 (1993) 409–486, https://doi.org/10.1111/j.1745-4557.1993.tb00269.x.
[32] L.F. Capitán-Vallvey, N. López-Ruiz, A. Martínez-Olmos, M.M. Erenas, A.J. Palma, Recent developments in computer vision-based analytical chemistry: A tutorial review, Anal. Chim. Acta 899 (2015) 23–66, https://doi.org/10.1016/j.aca.2015.10.009.